

## Effect of Flow Inlet or Outlet Direction on Air-Water Two-Phase Distribution in a Parallel Flow Heat Exchanger Header

Nae-Hyun Kim<sup>†</sup>, Do-Young Kim, Jin-Pyo Cho, Jung-Oh Kim, Tae-Kyun Park

Department of Mechanical Engineering, University of Incheon, Incheon, Korea

(Received February 20, 2008; Revision received March 7, 2008; Accepted June 12, 2008)

### Abstract

The air and water flow distributions are experimentally studied for a round header – ten flat tube configuration. Three different inlet orientation modes (parallel, normal, vertical) were investigated. Tests were conducted with downward flow configuration for the mass flux from 70 to 130 kg/m<sup>2</sup>s, quality from 0.2 to 0.6, non-dimensional protrusion depth ( $h/D$ ) from 0.0 to 0.5. It is shown that, for almost all the test conditions, vertical inlet yielded the best flow distribution, followed by normal and parallel inlet. Possible explanation is provided using flow visualization results.

*Key words:* Parallel flow heat exchanger, Header, Two-phase distribution, Air-water, Inlet orientation

### Nomenclature

$D$  : header inner diameter [m]  
 $G$  : mass flux [kg/m<sup>2</sup>s]  
 $h$  : protrusion depth [m]  
 $x$  : quality

### 1. Introduction

Brazed aluminium heat exchangers consist of flat tubes of 1 to 2 mm hydraulic diameter on the refrigerant-side, and louver fins on the air-side. They are seriously considered as evaporators of residential air conditioners due to the superior thermal performance as compared with conventional fin-tube heat exchangers. For a brazed aluminium heat exchanger, a number of tubes are grouped to one pass using a header to manage the excessive tube-side pressure drop by small channel size. To use the brazed aluminium heat exchanger as a refrigerant evaporator, it is very important to evenly distribute the two-phase refrigerant (especially the liquid) into each tube. Otherwise, the thermal performance is significantly deteriorated. According to Kulkarni et al.<sup>[1]</sup>, the performance reduction by flow mal-distribution could be as large as 20%. For an evaporator usage, the flat tubes

are installed vertically (with headers in horizontal position) to facilitate the air-side condensate drainage. In such a case, refrigerant may be supplied from three different directions as shown in Fig. 1. The refrigerant may be supplied parallel to the header, normal to the header and vertical to the header. The outlet may be located at the same side of the heat exchanger with the inlet or it may be located at the opposite side of the heat exchanger. In Fig. 1, the outlet is located at the same side of the heat exchanger. In addition to the inlet direction, many parameters, both flow and geometric, will affect the flow distribution in a parallel flow heat exchanger. Webb and Chung<sup>[2]</sup>, Hrnjak<sup>[3]</sup>, Lee<sup>[4]</sup> provide recent reviews on this subject.

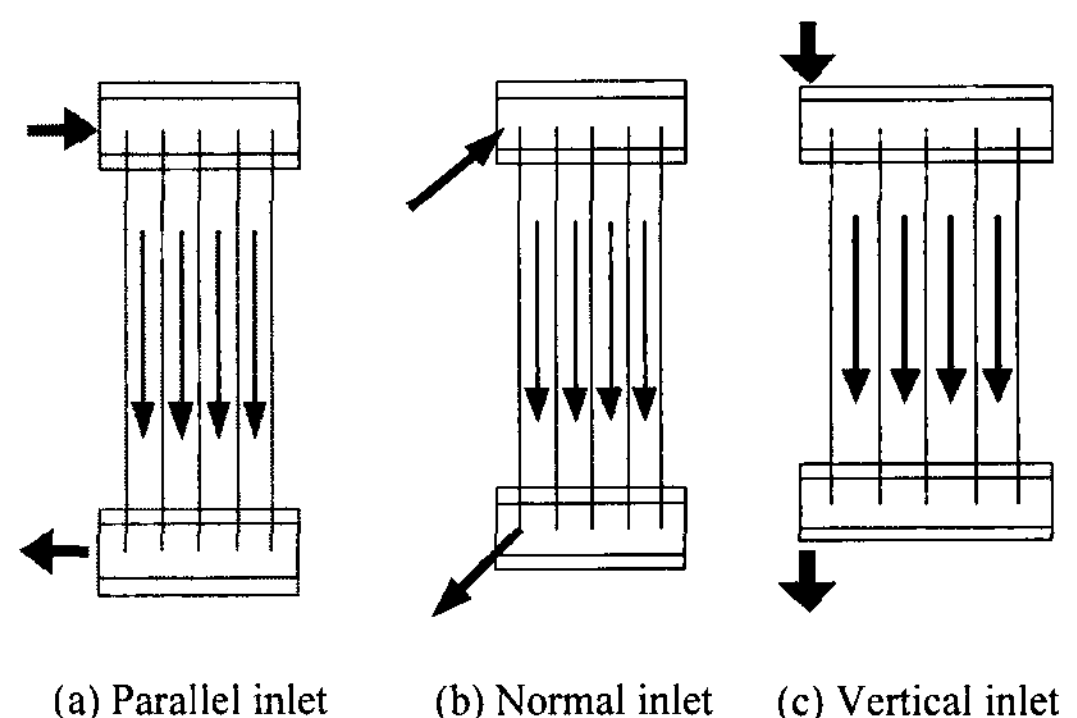


Fig. 1. Flow inlet orientations.

<sup>†</sup>Corresponding author. Tel.: +82 32 770 8420, Fax.: +82 32 770 8410  
 E-mail address: knh0001@incheon.ac.kr

The literature reveals several studies on the two-phase distribution in a header – branch tube configuration. Watanabe et al.<sup>[5]</sup> conducted a flow distribution study for a round header – four round branch tube upward flow configuration using R-11. At the inlet, flow was supplied parallel to the header. The flow distribution was highly dependent on the mass flux and the quality. Tompkins et al.<sup>[6]</sup> tested a rectangular header – fifteen flat tube downward flow configuration using air-water. The flow was supplied parallel to the header. The flow distribution was highly dependent on the mass flux and the quality. A better distribution was obtained at a lower mass flux (stratified flow regime). Vist and Pettersen<sup>[7]</sup> investigated a round header – ten round branch tube configuration using R-134a. Both upward and downward flow were tested. The flow was supplied parallel to the header. For the downward flow configuration, most of the liquid flowed through frontal part of the header. For the upward configuration, on the contrary, most of the liquid flowed through the rear part of the header. The liquid distribution improved as the vapor quality decreased. The mass flux had negligible effect on the flow distribution.

Lee and Lee<sup>[8]</sup> investigated the effect of the tube protrusion depth for a vertical rectangular header – five horizontal rectangular branch tube configuration using air-water. At the inlet, annular flow was supplied parallel to the header. The flow distribution was highly dependent on the protrusion depth. As the protrusion depth increased, more water flowed through the downstream part of the header. Cho et al.<sup>[9]</sup> investigated the effect of the header orientation (vertical and horizontal) and the refrigerant inlet pipe direction (parallel, normal, vertical) for a round header – fifteen flat tube configuration using R-22. The header mass flux was fixed at  $60 \text{ kg/m}^2\text{s}$ , and the quality varied up to 0.3. For a vertical header configuration, most of the liquid flowed through the frontal part of the header, and the effect of the inlet pipe direction was not significant. For a horizontal header, the flow distribution was highly dependent on the inlet pipe direction, and better distribution was obtained for the vertical or the normal flow configuration.

Koyama et al.<sup>[10]</sup> investigated the effect of varying the tube protrusion depth for a horizontal round header and six vertical flat tube configuration using R-134a. Tests were conducted for the downward configuration. The flow was supplied parallel to the

header. The protrusion depth was systematically varied, and the optimum configuration was found to be with front two tubes protruded to the center of the header and the remaining four tubes flush-mounted. Better liquid distribution was obtained at a lower vapour quality. Bowers et al.<sup>[11]</sup> investigated the effect of tube protrusion depth as well as the effect of the entrance length on the flow distribution for a downward configuration using R-134a. Their test section composed of horizontal round header and fifteen vertical flat tubes. The apparatus was equipped with an expansion valve, and expanded two-phase mixture was supplied to the test section through the entrance tube. For a short entrance length of 89 mm, the liquid distribution was relatively uniform with minor influence of protrusion depth, mass flux or quality. For a long entrance length of 267 mm, however, better distribution was obtained as the mass flux or the protrusion depth increased. The entrance tube was located parallel to the header.

Kim and Lee<sup>[12]</sup> also investigated the effect of tube protrusion depth for a round header and ten flat tube configuration using air and water. Both upward and downward configuration was tested. At the inlet, flow was supplied parallel to the header. For the downward flow configuration, most of the water flowed through frontal part of the header, and the effect of tube protrusion depth, mass flux or quality was significant. As the protrusion depth, mass flux or quality increased, more water was forced to rear part of the header. For upward flow configuration, however, most of the water flowed through rear part of the header, and the effect of the above mentioned parameters was insignificant. Rong et al.<sup>[13]</sup>, Bernoux et al.<sup>[14]</sup> provide flow distribution data for a plate heat exchanger geometry.

The above literature survey reveals that the two-phase flow distribution in a header – branch tube configuration is very complex. Many parameters, both geometric and flow, affect the results, and more data are needed on this subject. For the effect of inlet direction, Cho et al.'s<sup>[9]</sup> study is the only one available. However, their study has been conducted for a limited range of mass flux and quality, and the effect of protrusion depth has not been investigated. This study is a continuing effort succeeding Kim and Lee<sup>[12]</sup>, who investigated the air-water flow distribution in a parallel flow heat exchanger comprised of round header and ten branch flat tubes. The flow was supplied parallel to the header. In this study, the effect of inlet direction (parallel, normal, vertical as shown in Fig.

1) was investigated for downward flow configuration. The header mass flux and the quality were varied for  $70 \leq G \leq 130 \text{ kg/m}^2\text{s}$  and  $0.2 \leq x \leq 0.6$ . The effect of tube protrusion depth (non-dimensional protrusion depth,  $h/D = 0.0, 0.25, 0.5$ ) was also investigated. For all the test samples, inlet and outlet were located at the same side of the heat exchanger as illustrated in Fig. 1. One thing to note is that the practical protrusion depth of the brazed aluminium heat exchanger is  $h/D = 0.5$  to avoid clogging with brazing flux.

**2. Experimental Apparatus**

A schematic drawing of the experimental apparatus is shown in Fig. 2. The test section consists of the 17 mm ID upper and lower headers, which are 91 cm apart, and branch flat tubes inserted at 9.8 mm pitches. This configuration was chosen to simulate the actual parallel flow heat exchanger. The cross section of the present flat tube is shown in Fig. 3. The tube is made by extrusion from an aluminium stock. The hydraulic diameter is 1.32 mm, and the flow cross sectional area is  $12.24 \text{ mm}^2$ . The headers were made of transparent PVC for flow visualization. A 17 mm hole was machined longitudinally in a square PVC rod (25 mm x 25 mm x 400 mm), and ten flat holes for insertion of flat tubes were machined at the bottom. An aluminium plate, which had matching flat holes, was installed underneath the header as illustrated in Fig. 4. Flat tubes were secured, and the protrusion depth was adjusted using O-rings between the header and the aluminium plate. Transition blocks were installed in the test section to connect the flat tubes and the 6.0

mm ID round tubes. The round tubes served as flow measurement lines. At the inlet of the header, 1.0 m long copper tube having the same inner diameter as the header was attached. The tube served as the flow development section.

The water and air, whose flow rates are separately determined, are mixed in a mixer before the air-water mixture is introduced into the header. The flow rate of every other flat tube is measured by directing the air-water mixture to the separator in the flow measurement section. As shown in Fig. 2, two valves – one at the main stream, the other at the bypass stream – are installed at every other channel. Normally, main stream valves are open, and bypass stream valves are closed. To measure the flow rate at a certain channel, the main stream valve is closed, and the bypass valve is open. The flow measurement principle is illustrated in Fig. 5. To prevent possible flow pattern change before and during the measurement, the differential pressure between the inlet of the upper header and the transition section was maintained the same by controlling the valve in the transition section.

The pressure fluctuations during measurement were within 10% of the average value. The total water and air flow rates to the header were measured by a mass flow meter (accuracy:  $\pm 1.5 \times 10^{-6} \text{ kg/s}$ ) and a float type flow meter (accuracy:  $\pm 1\%$ ), respectively. The air flow rate out of the separator was measured

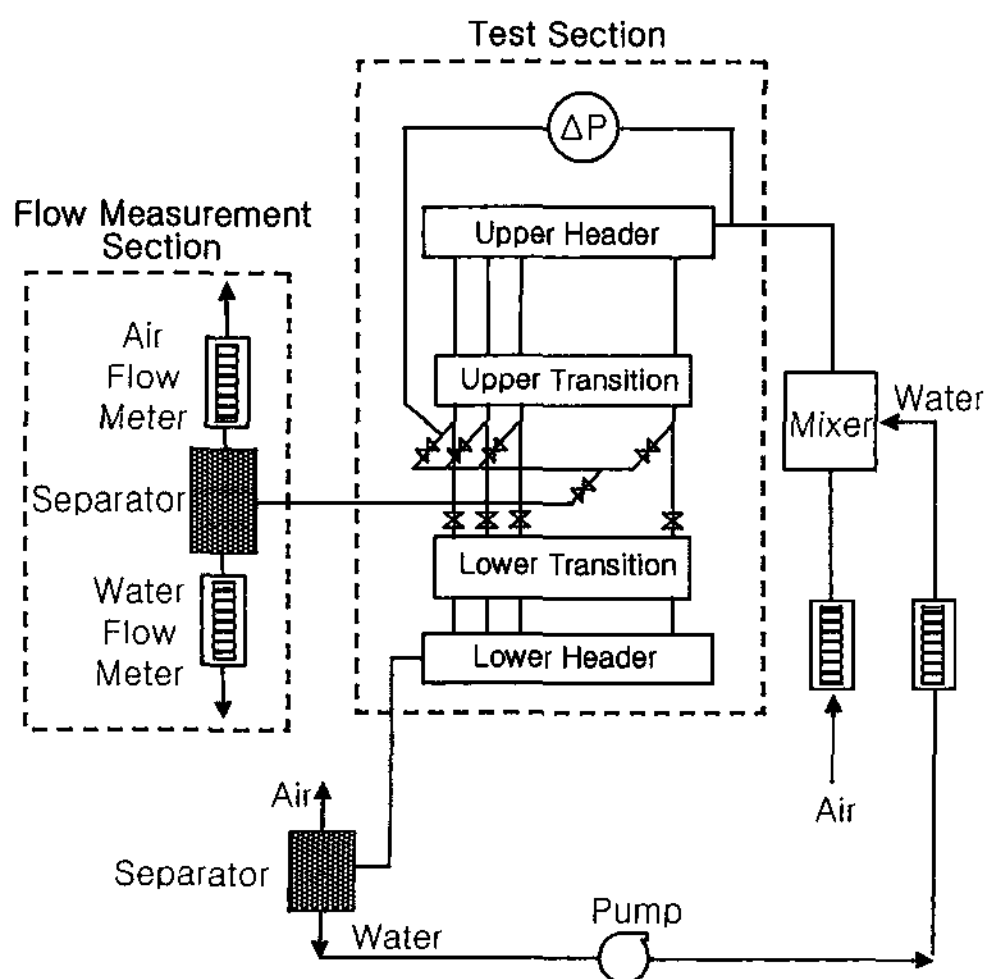


Fig. 2. Schematic drawing of the apparatus.

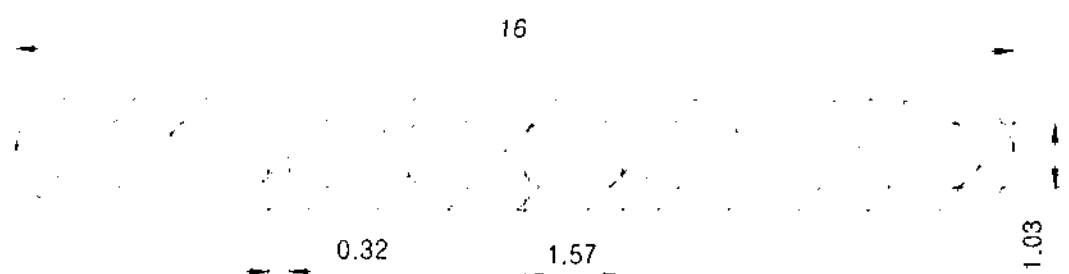


Fig. 3. Cross-sectional view of the flat tube used in this study (unit: mm)

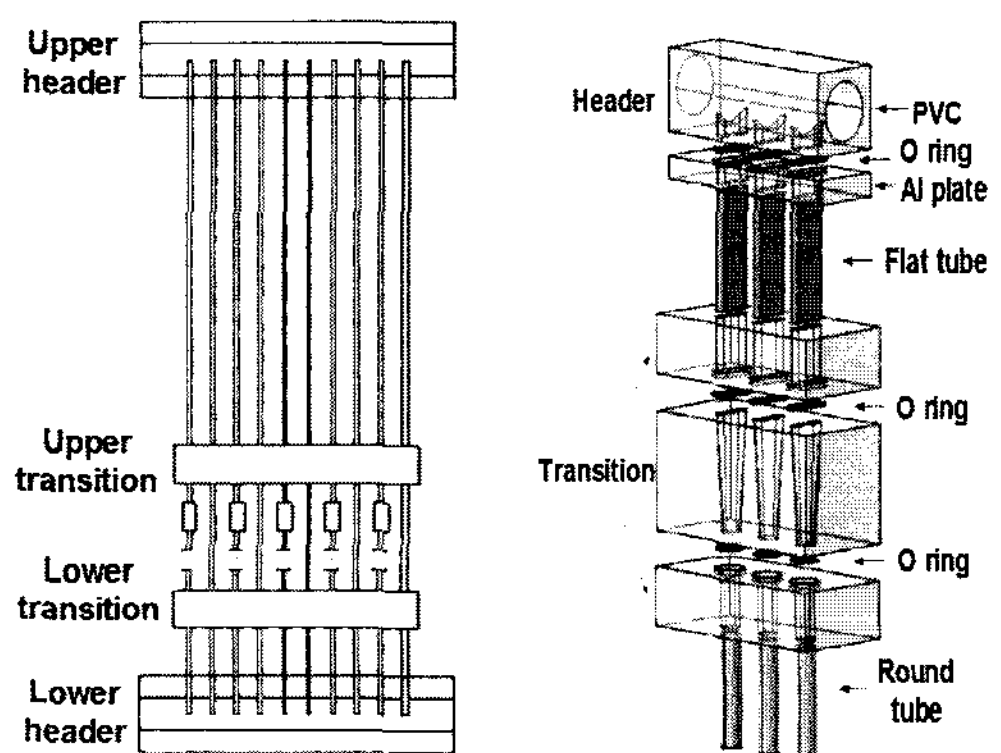


Fig. 4. Detailed drawing of the test section.

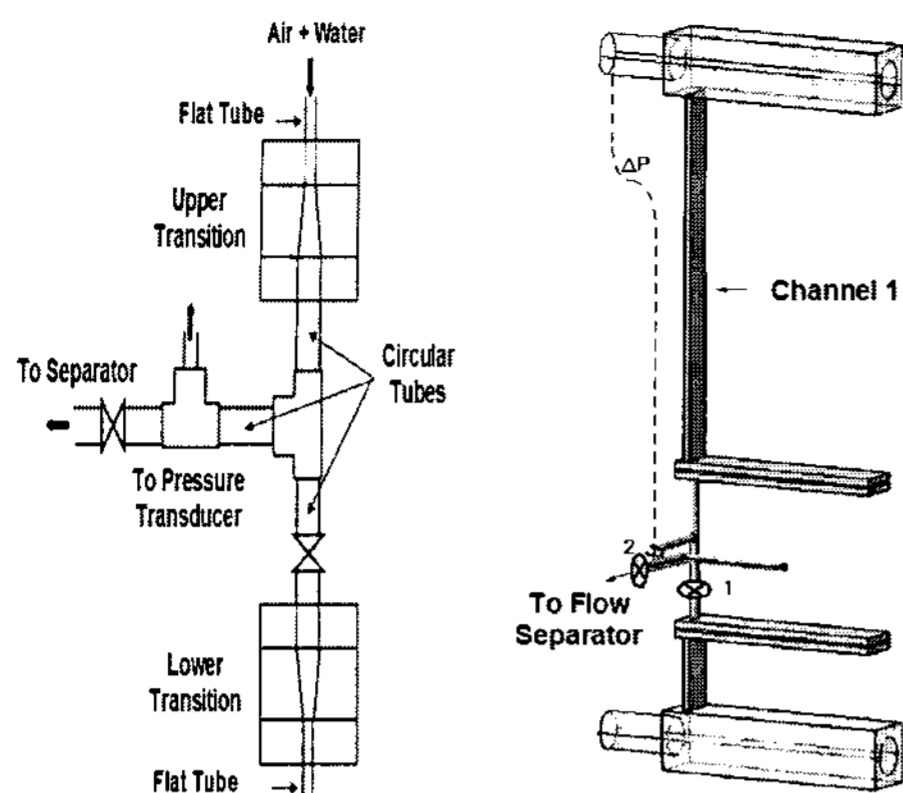


Fig. 5. Schematic drawing illustrating the flow measurement method.

by a float type flow meter (accuracy:  $\pm 1\%$ ), and the water flow rate out of the separator was measured by weighing the drained water in a graduated cylinder. During the whole series of tests, several runs were made to check the repeatability of the data. The data were repeatable within  $\pm 10\%$ . The maximum experimental uncertainty was  $\pm 10\%$  for the water flow rate measurement, and  $\pm 5\%$  for the air flow rate measurement. When the channel water or air flow rates were added and compared with the supplied water or air flow rates (for the channels where flow rates were not measured, the average values of the upstream and downstream channel flow rates were used), they agreed within 10%.

Tests were conducted with the inlet and the exit located at the same side of the test section (reverse configuration). The inlet and the exit may be located at the opposite side of the test section (parallel configuration). Kim and Lee<sup>[12]</sup> have shown that the water flow distribution is negligibly different between the reverse and the parallel configuration.

### 3. Results and Discussions

Typical water and air distribution data along with flow pattern are shown in Fig. 6 to 9. The ordinate of the Fig. 6 is the ratio of water or air flow rate in each tube to the average values. Fig. 6 shows the water and air flow ratio of the three different inlet directions for flush mounted configuration ( $h/D = 0.0$ ) at  $G = 100 \text{ kg/m}^2\text{s}$ ,  $x = 0.4$ . For parallel inlet configuration, significant amount of water flows through frontal channels. The water flow ratio of the first channel is 3.3, decreases to 0.6 at the third channel and remains approximately the same afterwards. The sketch of the

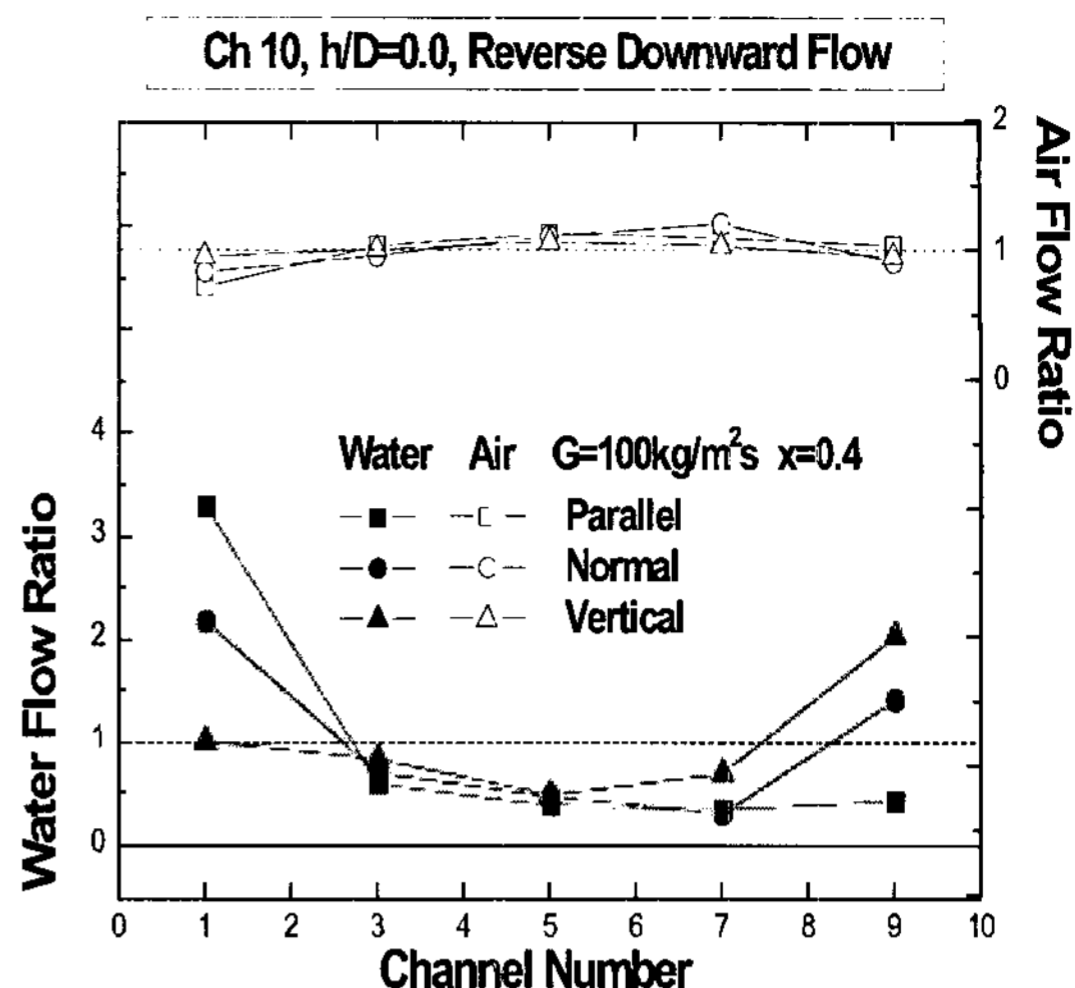


Fig. 6. Effect of inlet orientation on air and water flow distribution at  $G = 100 \text{ kg/m}^2\text{s}$ ,  $x = 0.4$ ,  $h/D = 0.0$ .

flow pattern shown in Fig. 7(a) shows thicker water film at frontal part of the header, which supports the flow distribution trend of Fig. 6.

For normal inlet configuration, compared with parallel inlet configuration, less water flows through frontal channels, and more water flows through latter part of the header. The water flow ratio of the first channel is 2.2, decreases to 0.4 at the seventh channel, and increases to 1.4 at the ninth channel. The accompanying flow pattern sketch in Fig. 7(b) illustrates that horizontally supplied water hits rear part of the header, and is forced to downstream along the wall of the header, yielding thicker water film at part of the header.

For vertical inlet configuration, compared with the parallel flow configuration, the water flow ratios of frontal channels significantly decrease and those of latter channels significantly increase. The water flow ratio of the first channel is 1.0, decreases to 0.6 at the fifth channel, and increases to 2.1 at the ninth channel. The accompanying flow pattern sketch in Fig. 7(c) illustrates that vertically supplied water hits bottom of the header, and is forced to downstream of the header, yielding thicker water films at latter part of the header. Calculation of the standard deviation of water flow ratio yielded 0.64 for the parallel inlet, 0.39 for the normal inlet and 0.30 for the vertical inlet, suggesting most uniform water distribution for the normal inlet configuration. Fig. 6 shows that air distribution is opposite to water distribution, although the difference is much less significant for air distribution.

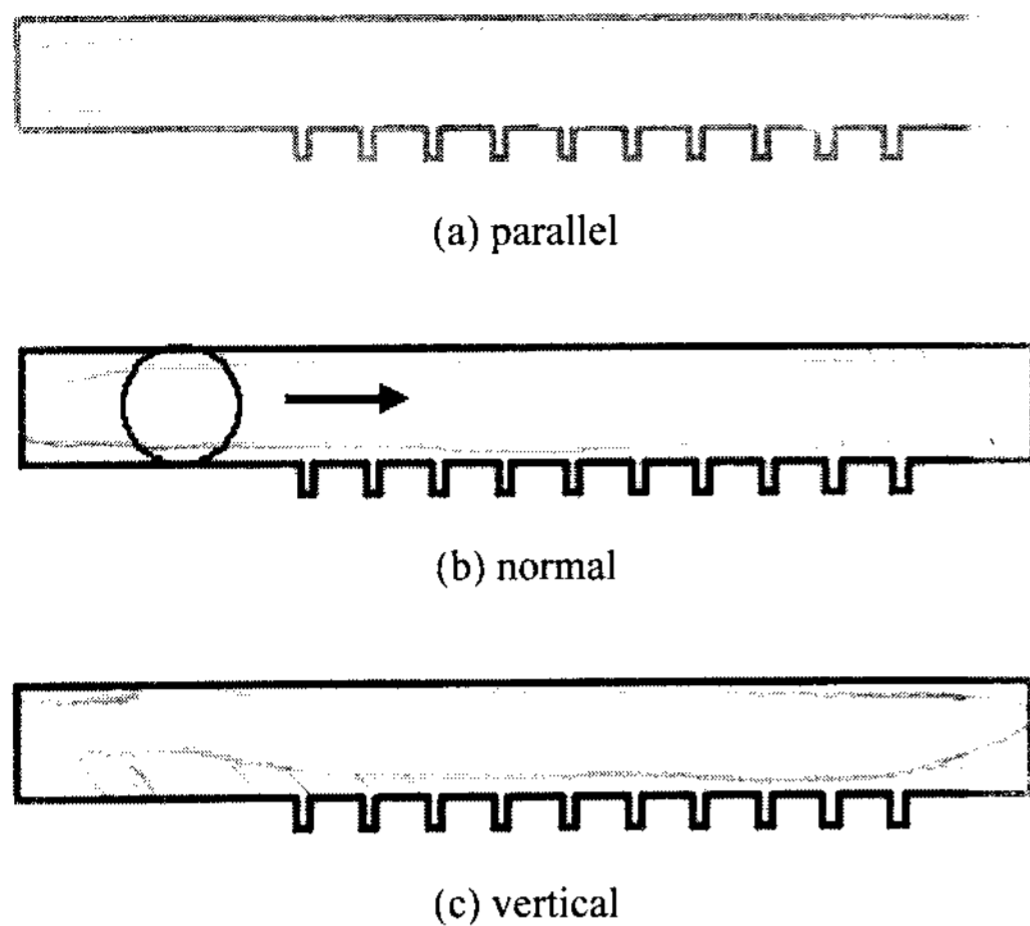


Fig. 7. Flow distribution sketches at  $G = 100 \text{ kg/m}^2\text{s}$ ,  $x = 0.4$ ,  $h/D = 0.0$ .

Calculation of the standard deviation of air flow ratio yielded 0.08 for the parallel inlet, 0.08 for the normal inlet, and 0.02 for the vertical inlet, suggesting most uniform air distribution for the normal inlet configuration. Although not shown in this manuscript, similar trend was observed at other mass fluxes or qualities.

Fig. 8 shows the water and air flow ratio for the tubes protruded to the center of the header ( $h/D = 0.5$ ) at  $G = 100 \text{ kg/m}^2\text{s}$ ,  $x = 0.4$ . For all the configurations, significant amount of water is forced to downstream of the header. For parallel inlet configuration, the water flow ratio of the first channel is 1.9, decreases to 0.2 at the third channel, and significantly increases to 2.2 at the ninth channel. The sketch of the flow pattern shown in Fig. 9(a) illustrates that part of the incoming water impinges at the first protrusion, some of it is sucked into the first tube, and the remaining water separates at the top. The separated water hits rear end of the header, and supplies water from downstream. The water, which bypassed the first protrusion, along with the water from upper part of the header, impinges at the second protrusion, part of it sucked in, separates at the top and hits the rear end of the header. The process continues until no water is available for separation at the top. The resultant water flow distribution yields more water supply through front and latter channels with minimal supply through middle-located channels.

For normal inlet configuration, compared with parallel inlet configuration, less water flows through frontal channels, and slightly more water flows

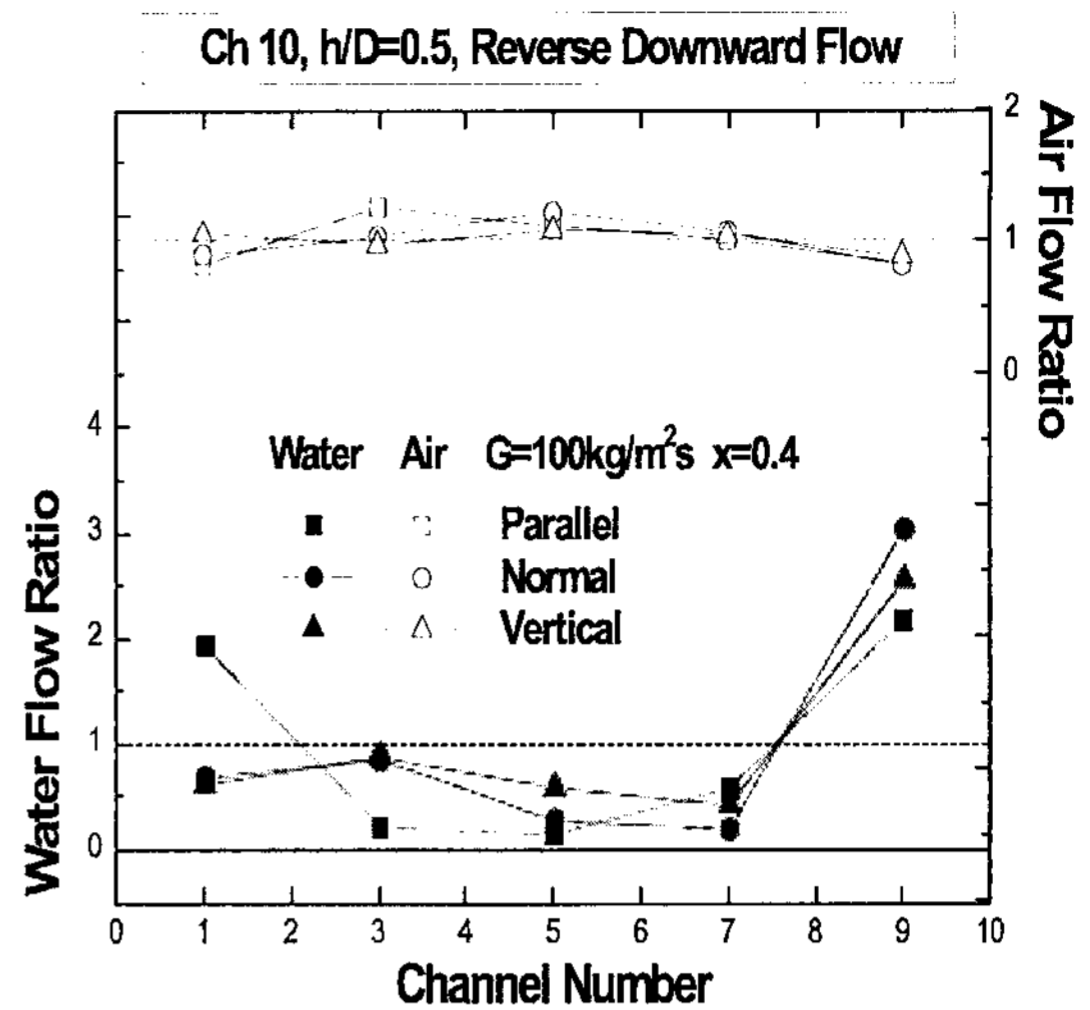


Fig. 8. Effect of inlet orientation on air and water flow distribution at  $G = 100 \text{ kg/m}^2\text{s}$ ,  $x = 0.4$ ,  $h/D = 0.5$ .

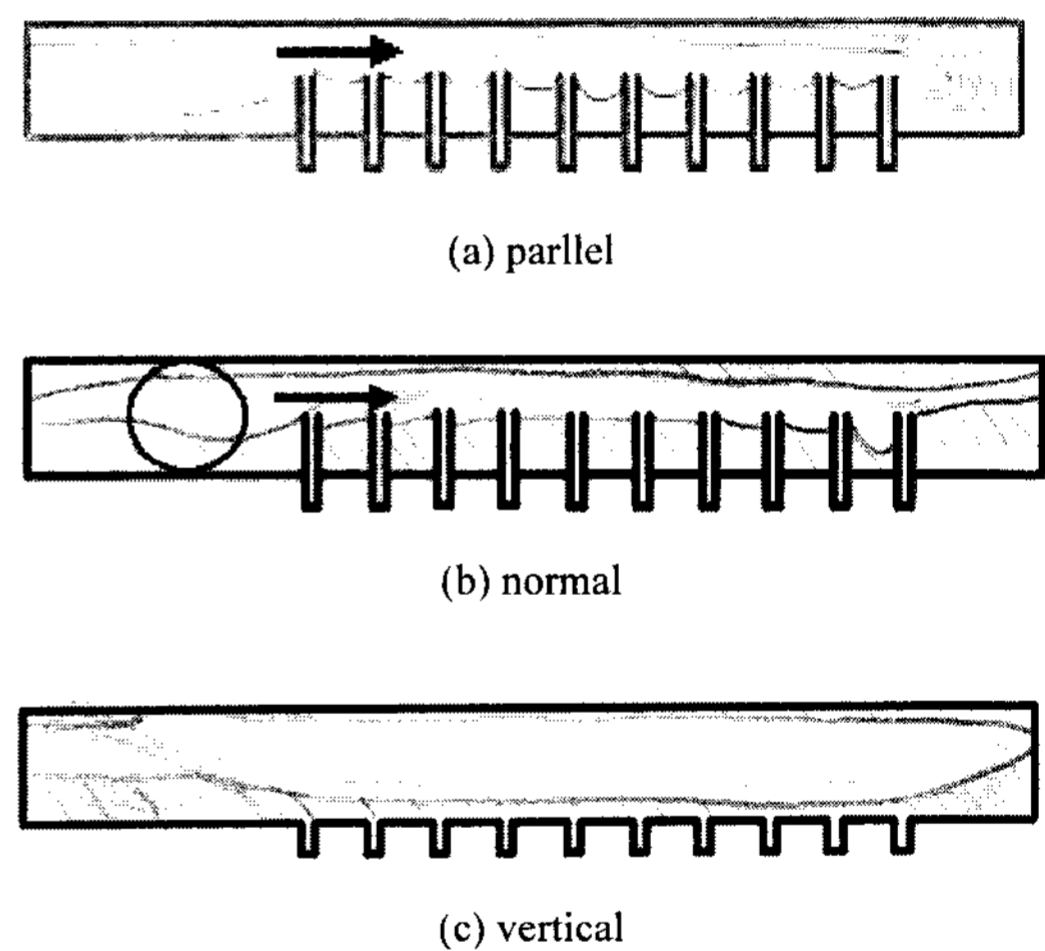


Fig. 9. Flow distribution sketches at  $G = 100 \text{ kg/m}^2\text{s}$ ,  $x = 0.4$ ,  $h/D = 0.5$

through latter part of the header. The water flow ratio of the first channel is 0.7, decreases to 0.4 at the seventh channel, and increases to 3.1 at the ninth channel. The accompanying flow pattern sketch in Fig. 9(b) illustrates that horizontally supplied water hits rear part of the header, and is forced downstream. Similar to the parallel inlet configuration, part of the incoming water impinges at the first protrusion, some of it is sucked in to the first tube and the remaining water separates at the top. The amount of separated water, however, was smaller than that of the parallel inlet configuration, which explains the smaller water flow ratio for the normal inlet configuration.

For vertical configuration, the water flow ratios are approximately the same as those of the normal flow configuration, except slightly less water flow ratio of 2.6 at the latter part of the header. The accompanying flow pattern sketch in Fig. 9(c) illustrates that vertically supplied water hits bottom of the header, and is forced downstream. Similar to the normal inlet configuration, part of the incoming water impinges at the first protrusion, some of it is sucked in to the first tube and the remaining water separates at the top. Calculation of the standard deviation of water flow ratio yielded 0.48 for the parallel inlet, 0.58 for the normal inlet and 0.44 for the vertical inlet, suggesting most uniform water distribution for the normal inlet configuration.

Fig. 8 shows that air distribution is opposite to water distribution. Calculation of the standard deviation of air flow ratio yielded 0.08 for the parallel inlet, 0.09 for the normal inlet and 0.04 for the vertical inlet, suggesting most uniform air distribution for the normal inlet configuration. Although not shown in this manuscript, similar trend was observed at other mass fluxes or qualities.

The standard deviations of the water and air flow ratios were calculated from the data, and the results are summarized in Table 1. Table 1 shows that, for almost all the cases, the standard deviation of the parallel inlet is the largest, followed by the normal inlet. The smallest value is obtained for the vertical inlet configuration, implying the best inlet configuration of the three.

#### 4. Conclusions

Effect of the inlet direction (parallel, normal, vertical) on flow distribution of the parallel flow heat exchanger consisting of round header and ten vertical channels was investigated using air-water for downward flow configuration. The header mass flux and the quality were varied for  $70 \leq G \leq 130$  kg/m<sup>2</sup>s and  $0.2 \leq x \leq 0.6$ . The effect tube protrusion depth was also investigated. For almost all the cases, best flow distribution was obtained for the vertical inlet configuration. It was observed that vertically supplied water hits bottom of the header, and is forced to downstream of the header, yielding more uniform distribution. Normal inlet was less effective in distributing the water than the vertical inlet, although it was much more effective than the parallel inlet. The vertical inlet was also the most effective in the distribution of the air.

Table 1. Standard deviation of the water and air ratio.

h/D	G (kg/m <sup>2</sup> s)	x	Standard Deviation					
			Parallel		Normal		Vertical	
			water	air	water	air	water	air
0.5	70	0.4	0.49	0.10	0.50	0.06	0.37	0.06
	100	0.2	0.41	0.15	0.44	0.15	0.31	0.13
	100	0.4	0.48	0.09	0.58	0.08	0.44	0.04
	100	0.6	0.73	0.06	0.56	0.03	0.20	0.01
	130	0.4	0.76	0.09	0.61	0.09	0.56	0.03
0.25	70	0.4	0.59	0.12	0.42	0.08	0.39	0.05
	100	0.2	0.58	0.26	0.41	0.18	0.27	0.10
	100	0.4	0.53	0.09	0.28	0.08	0.22	0.03
	100	0.6	0.57	0.06	0.36	0.07	0.13	0.01
	130	0.4	0.53	0.18	0.19	0.05	0.23	0.01
0.0	70	0.4	0.80	0.18	0.61	0.07	0.28	0.06
	100	0.2	0.70	0.31	0.48	0.18	0.42	0.15
	100	0.4	0.64	0.08	0.39	0.08	0.30	0.02
	100	0.6	0.56	0.07	0.40	0.04	0.10	0.03
	130	0.4	0.52	0.09	0.43	0.07	0.31	0.05

#### Acknowledgement

This research was supported by the University of Incheon Research Grant in 2007.

#### References

- [1] Kulkarni, T. Bullard, C. W. and Cho, K., 2004, Header design tradeoffs in microchannel evaporators, *Applied Thermal Engineering*, Vol. 24, pp. 759~776.
- [2] Webb, R. L. and Chung, K., 2004, Two-phase flow distribution in tubes of parallel flow heat exchangers, *Heat Transfer Engineering*, Vol. 26, pp. 3~18.
- [3] Hrnjak, P., 2004, Flow distribution issues in parallel flow heat exchangers, *ASHRAE Annual Meeting*, AN-04-1-2.
- [4] Lee, S. Y., 2006, Flow distribution behaviour in condensers and evaporators, *Proceedings of the 13<sup>th</sup> International Heat Transfer Conference*, KN-08, Sydney, Australia.
- [5] Watanabe, M., Katsuda, M. and Nagata, K., 1995, Two-phase flow distribution in multi-pass tube modeling serpentine type evaporator, *ASME/JSME Thermal Engineering Conf.*, Vol. 2, pp. 35~42.
- [6] Tompkins, D. M., Yoo, T., Hrnjak, P., Newell, T. and Cho, K., 2002, Flow distribution and pressure drop in micro-channel manifolds, *9<sup>th</sup> Int. Refrigeration and Air Conditioning Conference at Purdue*, R6-4.
- [7] Vist, S. and Pettersen, J., 2004, Two-phase flow

- distribution in compact heat exchanger manifolds, *Exp. Thermal Fluid Sci.*, Vol. 28, pp. 209~215.
- [8] Lee, J. K. and Lee, S. Y., 2004, Distribution of two-phase annular flow at header-channel junctions, *Exp. Thermal Fluid Sci.*, Vol. 28, pp. 217~222.
- [9] Cho, H., Cho, K. and Kim, Y., 2003, Mass flow rate distribution and phase separation of R-22 in multi-microchannel tubes under adiabatic condition, 1<sup>st</sup> Int. Conf. Microchannels and Minichannels, pp. 527~533.
- [10] Koyama, S., Wijayanta, A. T., Kuwahara, K., and Ikuda, S., 2006, Developing two-phase flow distribution in horizontal headers with downward microchannel branches, Proceedings of the 11<sup>th</sup> Int. Refrigeration and Air Conditioning Conference at Purdue, R142.
- [11] Bowers, C. D. Hrnjak, P. S. and Newell, T. A., 2006, Two-phase refrigerant distribution in a microchannel manifold, Proceedings of the 11<sup>th</sup> Int. Refrigeration and Air Conditioning Conference at Purdue, R161.
- [12] Kim, N.-H. and Lee, E.-R., 2008, Distribution of air-water annular flow in a header of a parallel flow heat exchanger, *Int. J. Heat Mass Transfer*, Vol. 57, pp. 977~992.
- [13] Rong, X., Kawaji, M. and Burgers, J. G., 1995, Two-phase header flow distribution in a stacked plate heat exchanger, FED-Vol. 225, Gas Liquid Flows, pp. 115~122.
- [14] Bernoux, P., Mercier, P. and Lebouche, M., 2001, Two-phase flow distribution in a compact heat exchanger, Proc. 3<sup>rd</sup> Int. Conf. Compact Heat Exchangers, pp. 347~352.